

Supporting Information:
Dynamics of Single Hydrogen Bubbles at Pt
Microelectrodes in Microgravity

Aleksandr Bashkatov^{*1}, Xuegeng Yang¹, Gerd Mutschke¹, Barbara Fritzsche²,
Syed Sahil Hossain¹ and Kerstin Eckert^{†1,2}

¹Institute of Fluid Dynamics, Helmholtz-Zentrum Dresden-Rossendorf, Bautzner
Landstrasse 400, Dresden, 01328 Germany

²Institute of Process Engineering and Environmental Technology, Technische
Universität Dresden, Dresden, 01062 Germany

*a.bashkatov@hzdr.de

†k.eckert@hzdr.de

Correlation with residual gravity and the pitch angle variation

In Figure S1, (a) the residual gravitational acceleration, (b) pitch angle θ , (c) bubble position X and (d) bubble radius R over time are exemplary documented for the micro- g phase of a parabola in 0.1 mol/L at -1.5 V. Beside the magnitude of the residual acceleration $g_{res} = \sqrt{g_{res,x}^2 + g_{res,y}^2 + g_{res,z}^2}$ (black line), also two components of it, $g_{res,x}/g$ (green line) and $g_{res,z}/g$ (orange line), are shown. All quantities are presented in relation to the terrestrial gravity g . Here, differently to Fig. 1(d) of the manuscript, the x -axis points in flight direction, the y -axis points left/right, and the z -axis points upward. The comparably smaller $g_{res,y}$ component is not shown here, in line with only rarely observed out-of-plane movements of the bubbles. Besides, the bubble radius R and the lateral displacement X are presented for five successively produced bubbles. Compared to Fig. 5 of the manuscript, the $R(t)$ and $X(t)$ data are resented here in a different form to better visualize the relation between lateral bubble displacement, bubble size and pitch angle and residual gravitational acceleration.

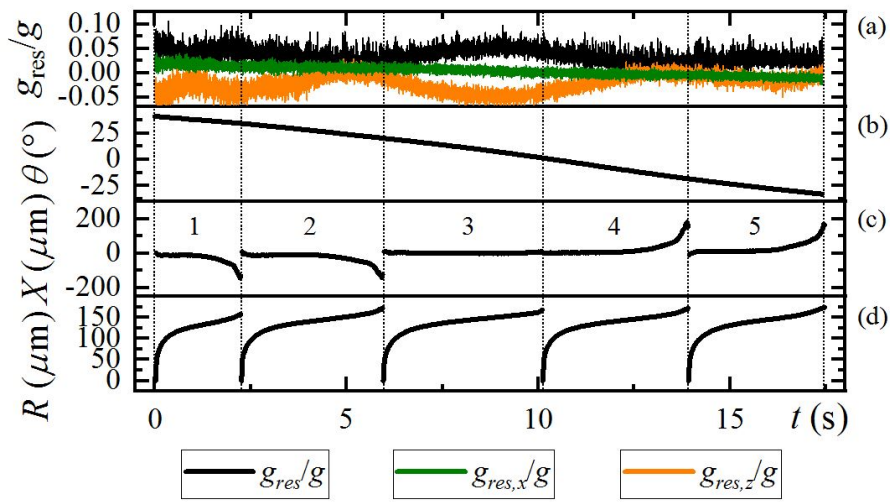


Figure S1: (a) the residual gravitational acceleration and components of it (see text), (b) pitch angle θ , (c) lateral bubble position X and (d) bubble radius R over time during the micro- g phase of a parabola in 0.1 mol/L at -1.5 V.

Due to the nature of the parabolic flight, the pitch angle θ is continuously changing from positive to negative values during the micro- g phase of a parabola. As can be seen from Fig. S1, the residual acceleration $g_{res,x}$ in the direction of flight clearly correlates with the pitch angle θ . The electrochemical cell is placed inside the plane such that the direction of flight coincides with the lateral direction x along the electrode in the optical plane. In Fig. S1 it can be clearly seen that the lateral bubble motion in x -direction is correlated with the x -component of the residual acceleration $g_{res,x}$ and the pitch angle θ . The bubble moves to the left, i.e. towards the cockpit, when the pitch angle is positive, and it moves to the right, i.e. towards the rear of the aircraft, when the pitch angle is negative. Despite at small pitch angles it takes longer for the bubbles to depart, the bubble size at departure is similar in all cases shown here, regardless of the pitch angle. Departure in all cases is accompanied eventually by a vertically upward motion of the bubble, which is important for the departure especially at small pitch angles. Despite the lateral movement observed due to $g_{res,x}$ is a specific feature of the parabolas, the influence of the residual acceleration in vertical direction $g_{res,z}$ is random. As the departure mainly seems to depend on the bubble size and the related forces acting on the bubble, we tend to say that the impact of the residual acceleration is weak only.

Electric current effect on the bubble lifetime

To reveal the effect of the electric current on the bubble growth under μg , the lifetime of individual bubbles T versus the averaged current \bar{I} is shown in Figure S2 for different potentials and concentrations. The dash-dotted lines correspond to a linear fit of the experimental points. Despite minor exceptions at 0.02 mol/L, a general trend is observed: The higher the current at fixed potential, the shorter the bubble lifetime. However, when the current is fixed, a larger potential increases the lifetime as the retarding forces increase.

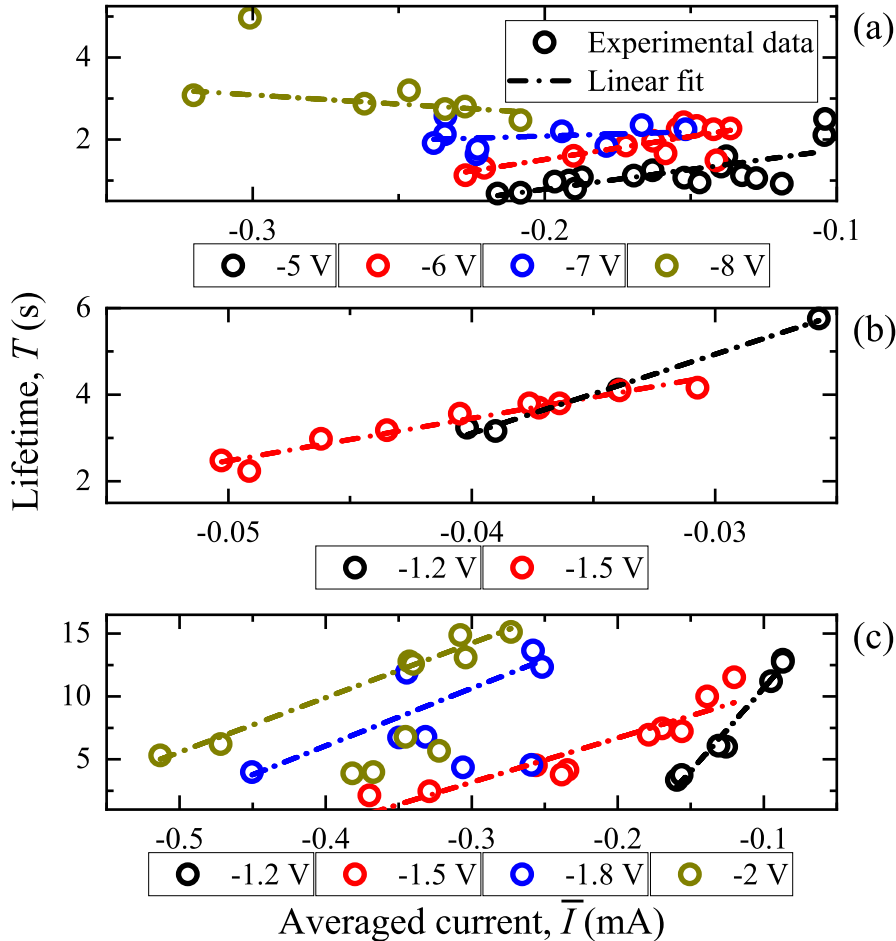


Figure S2: Lifetime of individual bubbles T vs. electric current \bar{I} averaged over bubble lifetime in (a) 0.02 mol/L at -5, -6, -7, -8 V; (b) 0.1 mol/L at -1.2, -1.5 V and (c) 0.5 mol/L at -1.2, -1.5, -1.8, -2 V. The dash-dotted lines show linear fits.

At fixed concentration, the slope of the linear fits varies with the potential. In subfigures (b) and (c), the slope is always positive while for a minority of data, i.e. the green circles in (a), even a slightly negative slope is observed. For the latter, more statistical data to quantify the impact from the pitch angle, residual gravity variation and bubble-bubble interaction are needed. Since the higher lifetime often makes it impossible to record several bubbles within one parabola, the case (c) represents a collection of the bubbles from different electrodes, parabolas and even days. For that reasons a number of outliers appeared at -1.8 and -2 V. Finally, we point to the much smaller current in (b), resulting from lower conductivity at such concentration and potential applied, compared to the other cases.

Unified bubble evolution

To further unify the results in view of the fluctuating bubble lifetime, $R(t)$ has been plotted over dimensionless time (t/T) and averaged over all bubbles studied at different potentials and concentrations. The averaged radius \bar{R} is plotted vs the dimensionless time t/T in double logarithmic form in Figure S3. This representation gets rid from perturbations like the pitch angle variation, aircraft vibrations, or the usage of different electrodes, which stretch the time needed to reach a detachment diameter. It shows the bubble evolution mechanism in its averaged state and displays a consistent effect of the potential on the growth rate.

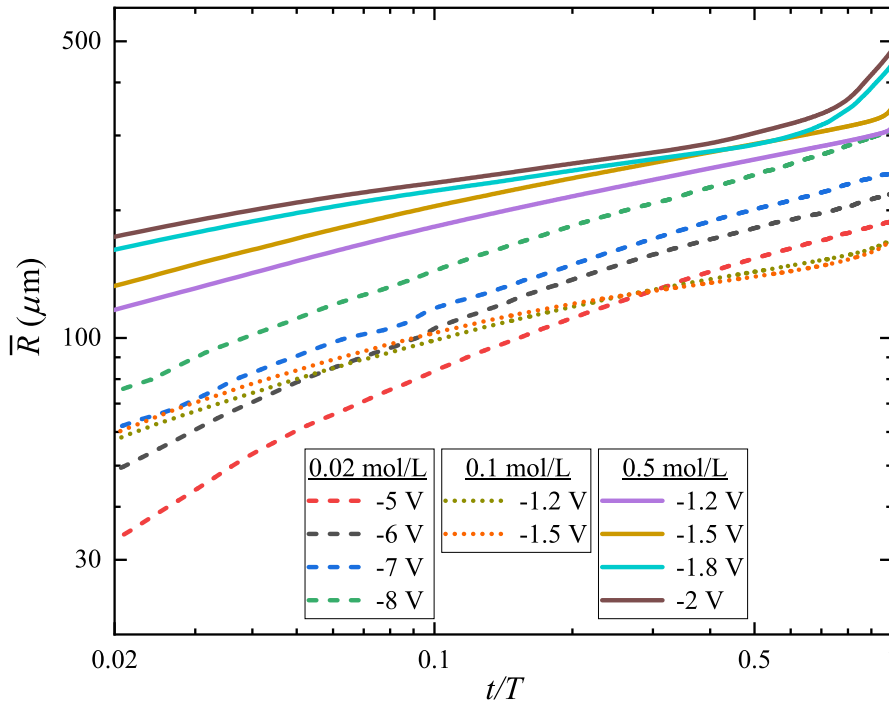


Figure S3: Radius \bar{R} , averaged over all bubbles grown at different potentials and concentrations, vs. dimensionless time t/T .

We next analyse the growth in terms the "growth coefficient" β and the power x of the power law $R = \beta \times (t/T)^x$. For 0.02 mol/L at -5...- 8 V, $\beta = [190, 220, 250, 310]$ and $\bar{x} = 0.33$ is the closest approximation, which works especially well within $t/T = 0.1...1$. In case of 0.1 mol/L we split the curves into two time slots: For $t/T = 0.02...0.1$ we obtain $\beta = 235$ and $\bar{x} = 0.35$, while for $t/T = 0.1...1$ $\beta = 160$, $\bar{x} = 0.19$ is found. For 0.5 mol/L we have a different behavior. At the potentials -1.2 V and -1.5 V we find $\beta = [310, 335]$ and $\bar{x} = 0.23$. For the higher potentials, -1.8 V and -2 V, we find in the window $t/T = 0.02...0.7$ values of $\beta = [330, 350]$, $\bar{x} = 0.18$, while for the final phase $t/T = 0.7...1$ the following holds: $\beta = [430, 460]$ and $\bar{x} \approx 1$. Thus at fixed electrolyte concentration the growth rate increases consistently upon increasing the potential. While the growth mechanism stays very similar for the low concentrations, 0.5 mol/L differs. Here, the last phase is characterized by the rapid enhancement in the growth rate with the time coefficient x close to 1 (at -1.8 V and -2 V). This is caused by the bubble displacement aside from the electrode and its inability to further detach due to downward forces or adhesion at the glass wall. This promotes an increase in current and coalescence rate, hence, finally growth rate. A similar effect could be found at -1.2 V and -1.5 V, however at considerably smaller extent.